07.1-13 INFLUENCE OF CADMIUM IONS ON THE LINEAR CRYSTAL GROWTH RATE OF POTASSIUM HALIDES: THE SYSTEM KBr-$CdBr_2$-H_2O. By D. Draganova, R. Koleva, Faculty of Chemistry, Sofia University, 1126 Sofia, Bulgaria.

This reports the effect of cadmium ions on the growth of potassium bromide crystals on the basis of the $R_{100}(C)$ and $R_{111}(C)$ curves, where R is the growth rate and C is the impurity concentration. The R-values were measured under stationery conditions by Bliznakov's method. The experimental data at 21°C, shown on fig. 1, as well as the data at 25 and 30°C, lead to the conclusion that cadmium ions are adsorbed and incorporated in KBr crystals according to two different mechanisms: I and II.

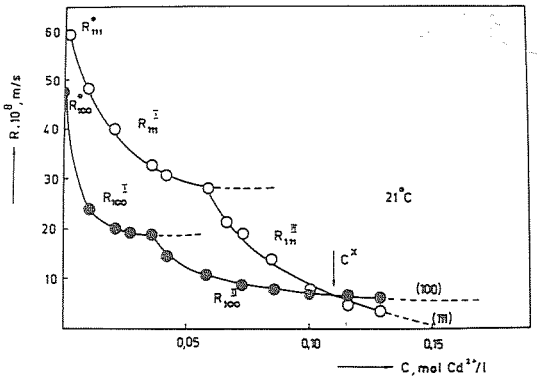

The mechanism I probably occurs through the adsorption of the complexes $CdBr_n^{2-n}$ (n<6), which turn into $CdBr_6^{4-}$ in the adlayer and enter the crystal lattice. Estimated from the R(C,T) curves the adsorption heats Q (kcal.mol^{-1}) are quite high: $Q^{I}_{100} \times Q^{I}_{111} = 14$. It seems that these Q-values include additional heat for the complex formation on the crystal surface.

The R(C)-I curves follow the equation of Bliznakov (Fortschr. Min. (1958) 36, 149), which permits the calculation of the surface diffusion activation energy for the adsorbed impurity complexes: 1075 cal for (100) and 720 cal for (111) KBr.

The mechanism II is a result of the formation of two-dimensional adsorption phases. That is why $Q^{II}_{111} > Q^{II}_{100}$ (Q^{II}_{111}=8,2; Q^{II}_{100}=5,1) and this leads to the habit transition (100)→(111) in the C-range of II, according to the relation given by Draganova:

$$\lg C^X = \text{const} + \frac{Q^{II}_{100} + Q^{II}_{111}}{2 \times 2.3\ RT}$$

Here C^X is the C-value, for which $R_{100}=R_{111}$ at the corresponding T.

These data seem to give a good explanation of two well known crystallographic phenomena: a) minute impurity traces stimulate the growth of more perfect single crystals - mechanism I with strong passivating effect, but without any change in the R_{100}/R_{111} ratio; b) habit modifications always occur at higher C-values. The succession of the action of mechanisms I and II and their different temperature dependence is the reason for the low concentration limits of the impurity habit changing activity.

07.2-01 MULTI-CELL-SIZE LATTICE MODELS APPLIED TO THE INTERPRETATION OF SMALL-ANGLE X-RAY SCATTERING DATA FOR CATALYSTS. By J. Goodisman and H. Brumberger, Dept. of Chemistry, Syracuse University, Syracuse, NY 13210.

Multi-cell-size models, employing spherical or cubic cells with different size distributions to represent the solid catalyst phase are used to interpret the observed small-angle X-ray scattering of two-phase (void-solid) Al_2O_3 catalysts. Theoretical scattering intensities are calculated from the correlation functions for these models, and the intensities are then numerically smeared for comparison with experimental data taken under "infinite slit" conditions. These models predict the bimodal form of the first moment of the slit-smeared intensity which appears to be appropriate for a number of catalysts.

07.2-02 THE STRUCTURES OF EQUILIBRIUM AND MELTING LENNARD-JONES CRYSTAL-MELT INTERFACES. By G. Bushnell-Wye and J. L. Finney, Crystallography Dept, Birkbeck College, Malet Street, London, WC1E 7HX, England, and A. Bonissent, Centre de Recherche sur les Mécanismes de la Croissance Cristalline, Campus de Luminy, Case 913, 13288 Marseille Cedex 2, France.

Monte Carlo calculations have been performed on the Lennard-Jones crystal-melt interface (the 0001 face of the h.c.p. system), both (a) slightly above and (b) at the triple point, to investigate the nature of the interface at equilibrium and on melting. The boundaries of the very large systems simulated (about 4500 atoms) were periodic along the interface. Ten layers of crystal were allowed to move under the Monte Carlo process, and these were bounded below by four further layers which remained fixed. The liquid region extended to about 20 layers above the interface, and its surface was either confined (to simulate constant volume) or free.

A hard sphere model of the interface was used as the starting configuration (Bonissent and Mutaftschiev, Phil. Mag. B35, 65, 1977). About 5 X 10^6 configurations have been calculated for the elevated temperature assembly, which begins to show the onset of melting. Unlike the behaviour observed in smaller assembly calculations (Bonissent, Gauthier and Finney, Phil. Mag. B39, 49, 1979), atoms moved in from both the liquid and crystal sides of the interface removing the density deficit observed at the interface in the earlier hard sphere models. Thus, in contrast to homogeneous simple liquids where the essential physics can be argued to be contained in the hard sphere structure, the severity of the packing constraints at a hard sphere interface seems to give rise to behaviour which is qualitatively different from the more realistic soft sphere case modelled here. Atom movements into the interfacial region from the crystal, together with plots of density profiles across the

crystalline layers at and below the interface, can be interpreted in terms of a roughening of the crystal surface. Trajectory plots normal to the interface show the onset of a cooperative melting process, and consequent distortions of the nearby crystal penetrate to 4-5 layers below the interface.

Results from constant volume and triple point calculations designed to suppress these movements will be presented, and the detailed structure of the equilibrium interface discussed.

07.2-03 METASTABLE PHASES IN THIN TIN AND LEAD FILMS AND THEIR OXIDES. By S.K. Peneva, K.D. Djuneva and D.D. Nihtianova, University of Sofia, Chemical Faculty, 1, Anton Ivanov Rd., Sofia 1126, Bulgaria.

RHEED studies have shown that diamond cubic structures with lattice parameters around the lattice parameter of silicon exist both in thin Sn and Pb films and in massive tin and lead solidified in vacuum $\sim 5.10^{-6}$ Torr, designated respectively as Sn(Si) and Pb(Si). It was found that three tin and lead intermediate oxides have almost identical structures. The initial oxides of Sn(Si) and Pb(Si) were identified as tin and lead analogues of SiO, demonstrating the similarity between tin and lead not only in the initial stages of crystallisation, but in the initial stages of oxidation (Peneva et al., J. Cryst. Growth, 53 (1981) in press). Depth selective Mössbauer Spectroscopy (DSMS) studies have shown a very high positive value of the isomeric shift δ of Sn(Si) + 4,42 $\pm$ 0,34 mm/s, relative to tin dioxide (Djuneva et al., Thin Solid Films 67 (1980) 371). Different other tin substructures were observed at different evaporation velocities, obtained by changing the temperature of the source, mostly in incommensurate states. Textured α-Sn films were grown with δ = + 2,2 $\pm$ 0,27 mm/sec, relative to tin dioxide. Films containing simultaneously textured α-Sn and tinI/tinII intermetallic compound, with structure resembling the structure of CuAu and isomeric shift δ (SnI.SnII(CuAu) = 1,00 $\pm$ 0,27 mm/s, relative to tin dioxide were also detected. It appears that the structure of tin and lead films depends on the structure of different metallic clusters coming from the vapours (e.g. Honig, J. Chem. Phys. 21 (1953) 573). Popel et al. (Fizika Metallov i Metallovedenie, Russan, 2, 38 (1974) present diffraction evidence for cluster structures in molten tin. Heating of thin tin films up to 400°C leads to complicated multiphase textures, with displaced 000 points of the reciprocal lattices of the various phases. There is tendency for segregation of tin atoms with $\sim$ similar electronic states into groups of similar substructures, as a rule in incommensurate states. Above 500°C, the number of incommensurate substructures decreases, and there is tendency for decrease of δ. The various tin substructures tend to form single crystal islands. It has been observed that Sn(Si) gets far less oxidized than the other tin substructures. SnO(SiO) is the common initial oxide observed as islands on all types of thin tin films and in chemically vapour grown tin oxide films (TOF) (e.g. Abstr. ICCG-6, Moscow, 1980, 4, 253; J. Crystal Growth, 73 (1981) in press). RHEED and DSMS show that there are at least two mechanisms for further oxidation of SnO(SiO). The first mechanism is a regular phase transformation of SnO(SiO), a = 6,42 Å $\pm$ 0,05 Å into tin perovskite (pseudocubic) a = 7,48 Å $\pm$ 0,07 Å, or phase transformations of incommensurate SnO(SiO) into incommensurate perovskites, resembling the data of $CaSnO_3$, ASTM 3-0755. The second mechanism resembles very much the oxidation of titanium oxides. The observed interplanar distances in the row of incommensurate SnO_x structures are very similar to the interplanar distances of the different TiO_x, as given in the ASTM Tables.

07.2-04 ANALYSIS OF AIR EXPOSED SURFACE OF Cr, Fe and Al. By Fumio Watari and J. M. Cowley, Arizona State University, Dept. of Physics, Tempe, AZ 85281 USA

When the fresh surface of Cr, Fe and Al is exposed to air at 300°K, an oxide layer is formed over the surface. This is confirmed and its composition and structure can be analyzed by scanning transmission electron microscopy (STEM) with the specimens prepared either outside the microscope or by in-situ evaporation followed by air-exposure.

The thin films prepared by evaporation, then exposed to air outside the microscope, had their thickness changed systematically from 10 to 1500 Å. Without use of a supporting film and with the availability of relatively larger uniform area and easier control of thickness, they provide suitable conditions for quantitative analysis. In order to compare the specimens before and after air exposure and to eliminate the possible influence of substrate and water, in-situ evaporation was performed in vacuum better than 1×10^{-7} Torr. Besides the use of carbon film as substrate, α whisker of CuO with about 200Å diameter was also used and metal deposits were crystallized around it.

In all these metals, oxide formation was detected by electron energy loss spectroscopy. The increase of oxygen pick-up in aging at 300°K was observed in Fe. The composition of oxide layer is roughly 0.5 and 1 in ratio of cation/anion and the thickness about 10Å and 100Å for Cr and Fe respectively. Microdiffraction with the probe size about 15Å in diameter shows diffuse scattered pattern for some time after specimen preparation, suggesting an amorphous structure. The intensity profile for the initial state of oxide structure was taken from selected area diffraction patterns using the line scan mode. Radial distribution analysis showed the cation-cation nearest neighbor distance to be about 3.4Å for Fe and Cr.